



Experimental Laminin 332 Mucous Membrane Pemphigoid Critically Involves C5aR1 and Reflects Clinical and Immunopathological Characteristics of the Human Disease

Eva Nina Heppe^{1,7}, Sabrina Tofern^{1,7}, Franziska S. Schulze¹, Akira Ishiko², Atsushi Shimizu², Christian Sina³, Detlef Zillikens⁴, Jörg Köhl^{5,6}, Stephanie Goletz¹ and Enno Schmidt^{1,4}

Mucous membrane pemphigoid is an autoantibody-mediated disease predominantly affecting the oral cavity, pharynx, and conjunctiva. Conjunctival lesions may lead to impaired vision and, finally, blindness. About 25% of mucous membrane pemphigoid patients generate autoantibodies against the $\alpha 3$ chain of laminin 332 (LAM $\alpha 3$), a structural protein of epidermal/epithelial basement membranes. Here, we established a mouse model by the passive transfer of rabbit IgG against the murine homologs of two immunodominant fragments in adult C57BL/6 mice (mLAM $\alpha 3$). After repeated subcutaneous injections of anti-mLAM $\alpha 3$ IgG erosions and crusts occurred predominantly around the snout, eyes, and on ears. Conjunctival and oral/pharyngeal lesions with subepithelial splitting were found in 80% and 100% of mice, respectively. In contrast, disease development was abrogated in FcR γ chain-deficient mice and markedly reduced in C5aR1-deficient mice. Furthermore, wild-type mice injected with anti-mLAM $\alpha 3$ F(ab')₂ were completely protected. Our findings suggest a crucial codominant role of FcR γ and complement activation of the anti-mLAM $\alpha 3$ IgG-induced mouse model of mucous membrane pemphigoid. This model will help further discover the pathomechanisms of this devastating disease. Furthermore, it may be of use to explore the effect of urgently needed more specific anti-inflammatory mediators on mucosal and skin lesions in autoantibody-mediated diseases.

Journal of Investigative Dermatology (2017) **137**, 1709–1718; doi:10.1016/j.jid.2017.03.037

INTRODUCTION

Pemphigoid diseases are a heterogeneous group of prototypic autoantibody-mediated disorders (Schmidt and Zillikens, 2013). Common features are the high morbidity, the well-defined target antigens, and the lack of specific anti-inflammatory therapies. Mucous membrane pemphigoid (MMP) is the second most frequent subepidermal blistering disease, with an estimated incidence of

about 1.3–2.0 per million per year in France and Germany and a prevalence of 24.6 per million in 2014 in Germany (Bernard et al., 1995; Bertram et al., 2009; Hübner et al., 2016).

MMP has been defined as a disease with autoantibodies against components of the dermal-epidermal junction (DEJ) and predominant mucosal involvement (Chan et al., 2002). In particular, conjunctival lesions are associated with an enormous health burden since scar formation induces visual impairment and, finally, blindness (Higgins et al., 2006). About 75% of MMP patients generate autoantibodies against BP180 (type XVII collagen) (Bernard et al., 1992; Oyama et al., 2006; Schmidt et al., 2001). In 20–25% of patients, autoantibodies target laminin 332, formerly termed laminin 5 and epiligrin (Bernard et al., 2013; Domloge-Hultsch et al., 1992; Leverkus et al., 1999; Schmidt et al., 2001). In less than 5% of MMP patients, reactivity against $\alpha 6$ integrin, $\beta 4$ integrin, and type VII collagen has been described (Schmidt and Zillikens, 2013).

Anti-laminin 332 MMP may be associated with a solid malignancy in about 30% of patients (Egan et al., 2001; Leverkus et al., 1999), with more extensive disease (Bernard et al., 2013), and with a higher frequency of oral mucosa and skin involvement (Amber et al., 2016).

Laminin 332 is composed of the $\alpha 3$ (LAM $\alpha 3$), $\beta 3$, and $\gamma 2$ chain encoded by three different genes, LAMA3, LAMB3, and

¹Lübeck Institute for Experimental Dermatology (LIED), University of Lübeck, Lübeck, Germany; ²Department of Dermatology, School of Medicine, Faculty of Medicine Toho University, Tokyo, Japan; ³Molecular Gastroenterology, Medical Department 1, University of Lübeck, Lübeck, Germany; ⁴Department of Dermatology, University of Lübeck, Lübeck, Germany; ⁵Institute for Systemic Inflammation Research, University of Lübeck, Lübeck, Germany; and ⁶Division of Immunobiology, Cincinnati Children's Hospital Medical Center and University of Cincinnati College of Medicine, Cincinnati, Ohio, USA

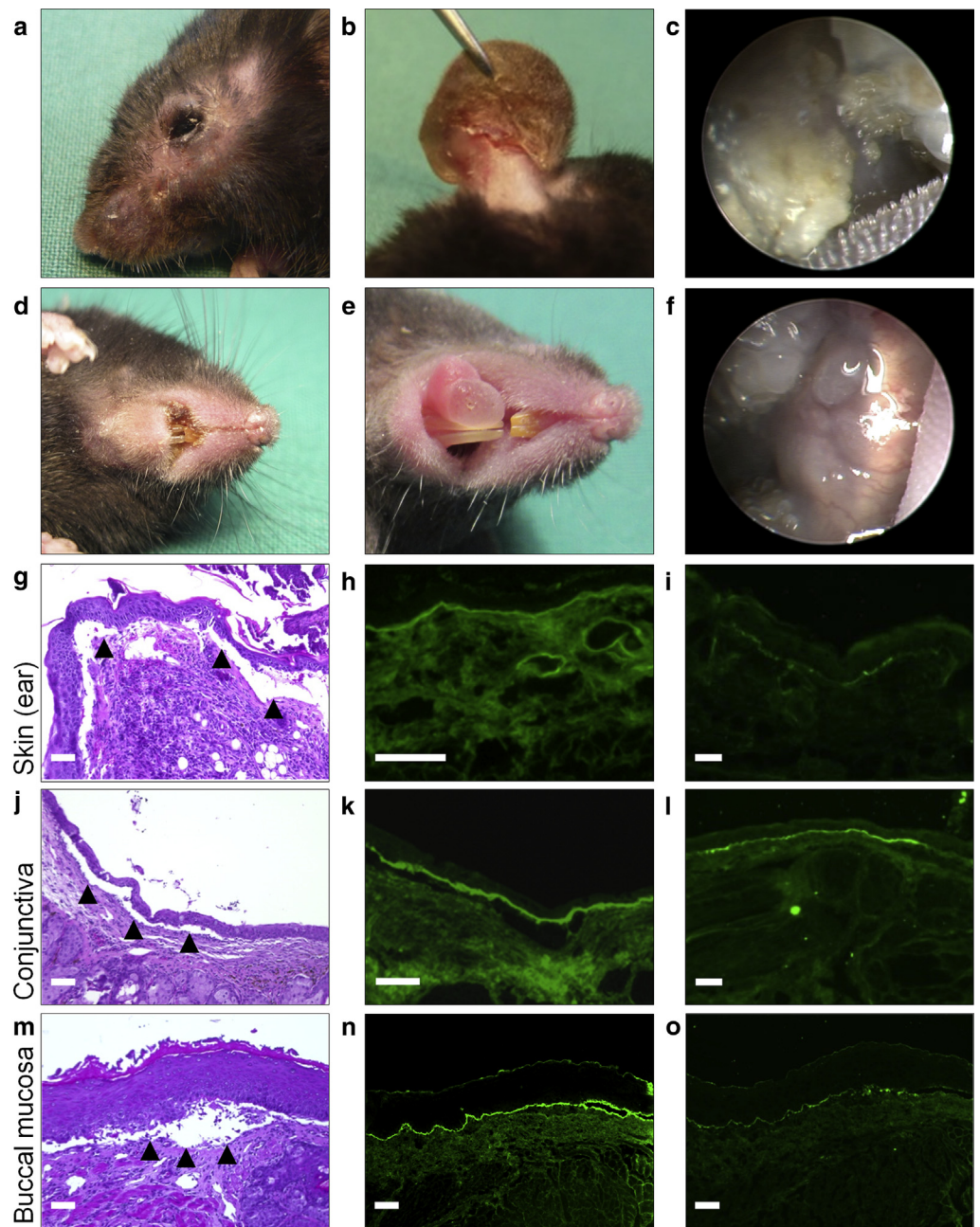
⁷These authors contributed equally to this work.

Correspondence: Enno Schmidt, Lübeck Institute for Experimental Dermatology (LIED), University of Lübeck, Ratzeburger Allee 160, D-23538, Lübeck, Germany. E-mail: enno.schmidt@uksh.de

Abbreviations: BP, bullous pemphigoid; c-term, C-terminal; DEJ, dermal-epidermal junction; EBA, epidermolysis bullosa acquisita; LAM $\alpha 3$, $\alpha 3$ chain of laminin 332; mid, middle portion; mLAM $\alpha 3$, murine $\alpha 3$ chain of laminin 332; MMP, mucous membrane pemphigoid

Received 17 January 2017; revised 23 March 2017; accepted 27 March 2017; accepted manuscript published online 26 April 2017

Figure 1. C57BL/6 mice injected with anti-mLAM α 3 IgG recapitulate major clinical, histopathological, and immunopathological findings of anti-laminin 332 MMP. Rabbit IgG against mLAM α 3 was injected at a dose of 7.5 mg/mouse subcutaneously into the neck of C57BL/6 mice ($n = 13$) every second day for 12 days. (a–f) Mice developed erosions and crusts (a) around the eyes, (b) on the ears and (d) snout, and on neck and feet (not shown). Erosions and blisters were seen on the (e) tongue, (f) oral mucosa, and (c) pharynx. (g, j, m) Histopathology of lesional biopsy samples of ear skin, conjunctiva, and buccal mucosa. Extensive subepidermal splits and dense infiltrate of inflammatory cells in the upper dermis are seen (hematoxylin and eosin staining). Arrowheads indicate subepidermal splitting. Direct immunofluorescence microscopy of perilesional biopsy samples of (h, i) ear skin, (k, l) conjunctiva, and (n, o) buccal mucosa. Linear deposits of (h, k, n) rabbit anti-mLAM α 3 IgG and (i, l, o) murine C3 along the basal membrane zone are present. Scale bars = 50 μ m. mLAM α 3, murine α 3 chain of laminin 332; MMP, mucous membrane pemphigoid.



LAMC2 (see [Supplementary Figure S1a](#) online). In most patients with anti-laminin 332 MMP, autoantibodies recognize the α 3 chain of laminin 332 (Kirtschig et al., 1995; Lazarova et al., 2001). Laminin 332 is central for hemidesmosome formation and interacts with BP180, type VII collagen, and α 6 β 4 integrin (Borradori and Sonnenberg, 1999; Hamill et al., 2010). Its pivotal role in the integrity of basement membranes is reflected by mutations in one of the three genes resulting in junctional epidermolysis bullosa and by autoantibody binding leading to anti-laminin 332 MMP (Domloge-Hultsch et al., 1992; Fine et al., 2014).

Here, we describe a mouse model of anti-laminin 332 MMP that is based on the passive transfer of antibodies against murine LAM α 3 (mLAM α 3) in adult C57BL/6 mice.

This model reflects major clinical and immunopathological characteristics of the human disease, that is, (i) severe oral and pharyngeal lesions, (ii) conjunctival involvement, (iii) linear deposits of IgG and C3 at the DEJ, (iv) subepidermal split formation with a dense inflammatory infiltrate below the DEJ by histopathology, and (v) splitting in the lower lamina lucida by electron microscopy.

RESULTS AND DISCUSSION

Different animal models have been developed that reflect major clinical and immunopathological characteristics of the human diseases bullous pemphigoid (BP) (Liu et al., 1993; Nishie et al., 2007; Schulze et al., 2014; Yamamoto et al., 2002) and epidermolysis bullosa acquisita (EBA)

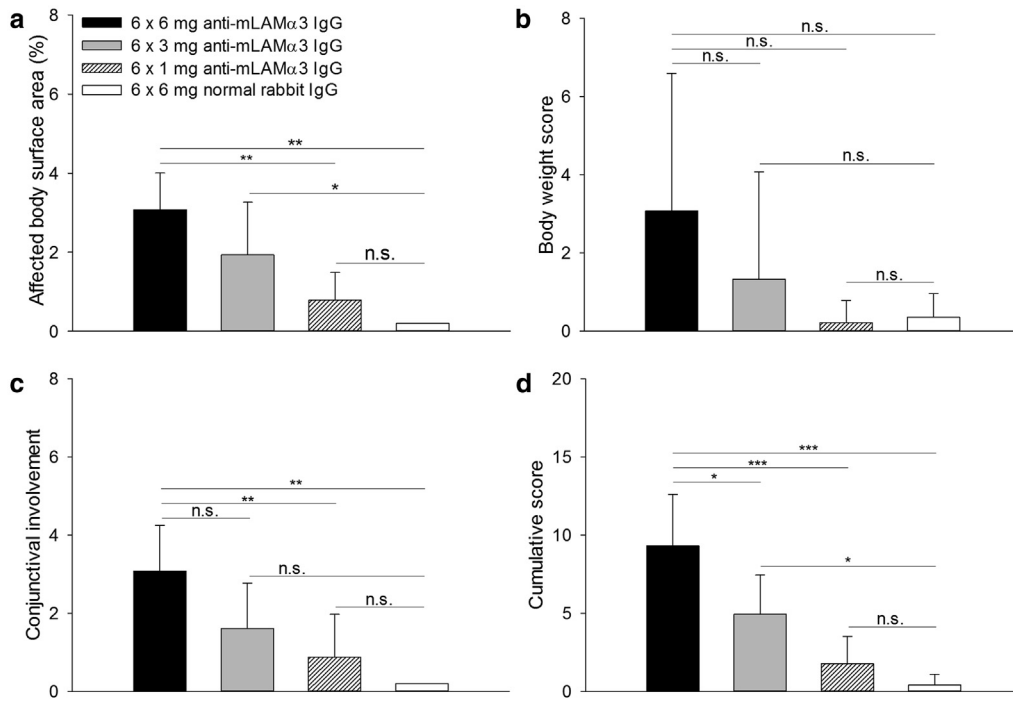


Figure 2. Disease activity correlates with the amount of injected anti-mLAM α 3 IgG. (a–d) The extent of (a) skin and (c) conjunctival lesions and (d) the cumulative disease score analyzed during the entire experiment are significantly higher when IgG at doses of 6 mg/mouse ($n = 7$) was injected on days 0, 2, 4, 6, 8, and 10 compared with 3 mg/mouse ($n = 7$) and 1 mg/mouse ($n = 7$). As control, adult C57BL/6 mice ($n = 3$) were injected on the same days with IgG at a dose of 6 mg/mouse. (b) Changes in body weight reflecting the extent of oral lesions were apparent but not significant between the groups. Bars represent the mean + standard deviation. One-way analysis of variance, with Holm-Sidak posttest when analysis of variance result was significant. * $P < 0.01$, ** $P < 0.001$, *** $P < 0.0001$. mLAM α 3, murine α 3 chain of laminin 332; n.s., not significant.

(Sitaru et al., 2006; Sitaru et al., 2005; Woodley et al., 2005). However, the search of an animal model for MMP that mirrors major clinical features of the human disease, that is, a variable inflammatory infiltrate in the upper dermis/mucosa and involvement of the oral cavity, pharynx, and conjunctiva, has intrigued researchers in the field for years.

Characterization of anti-mLAMA α 3 IgG

Here, by epitope mapping of laminin 332 using sera of anti-laminin 332 MMP patients ($n = 20$) and various recombinant forms covering the entire human LAM α 3, we initially identified two immunodominant regions at the N- and C-terminus of human LAM α 3 (detailed in the Supplementary Materials online, Supplementary Figure S1). LAM α 3 is targeted by most patients with anti-laminin 332 MMP, and the C-terminal region has previously been reported as its immunodominant target in anti-laminin 332 MMP (Kirtschig et al., 1995; Lazarova et al., 2001).

Subsequently, we generated rabbit IgG against the recombinant murine homologs of the two immunodominant human LAM α 3 fragments (see Supplementary Figure S2b online). Anti-mLAM α 3 IgG recognized the recombinant mLAM α 3 fragments by immunoblotting, bound along the dermal side of murine salt-split skin by indirect immunofluorescence microscopy, and labelled the interface of the lower lamina lucida and the upper portion of the lamina densa by indirect immunogold electron microscopy, as known for autoantibodies in patients with anti-laminin 332 MMP (see Supplementary Figure S2c–e) (Domloge-Hultsch et al., 1994; Domloge-Hultsch et al., 1992; Hsu et al., 1997; Kirtschig et al., 1995).

Transfer of anti-mLAMA α 3 IgG induces MMP-like clinical lesions in adult mice

Repeated injections of anti-mLAM α 3 IgG in adult C57BL/6 mice resulted in severe oral and pharyngeal blisters and

erosions as seen by endoscopy leading to considerable weight loss (Figure 1c, 1e, 1f, and 1m). In addition, split formation developed on the conjunctiva and esophagus (Figure 1j, Supplementary Figure S4j) and, on the skin, lesions appeared around the eyes and snout and on ears (Figure 1a, 1b, and 1d). Lesions around the eyes and snout are also seen in the antibody transfer mouse models for EBA and BP; however, they were more pronounced in our model (Schulze et al., 2014; Sitaru et al., 2005). We speculate that the expression of LAM α 3 in these areas is particularly high. Like in the models of EBA and BP, fur-covered body sites are less frequently involved, most likely because of an increased stability of the DEJ by the numerous hair follicles.

In human anti-laminin 332 MMP, oral involvement is present in almost all patients and ocular and skin lesions in about half of patients (Amber et al., 2016). The clinical presentation of the anti-laminin 332 mouse model established here clearly differs from the previously described mouse model, in which neonatal BALB/c mice developed subepithelial lesions of skin and nasal and oral mucosa 24–48 hours after the injection of rabbit IgG generated against human laminin 332 (Lazarova et al., 1996). In this model, no conjunctival lesions were reported and no inflammation was seen by lesional histopathology, which is in sharp contrast to the great majority of MMP patients. In contrast, subepithelial blisters on conjunctiva and cornea, as well as eyelid changes and periorbital hair loss, were reported after regional injection of rabbit anti-laminin 332 IgG in adult BALB/c mice (Lazarova et al., 2007).

In addition, in previously described models of EBA and BP, no conjunctival lesions were observed, and oral lesions were mild or absent (Ishii et al., 2011; Liu et al., 1993; Nishie et al., 2007; Schulze et al., 2014; Sitaru et al., 2005, 2006; Woodley et al., 2005). The clinical differences in the latter

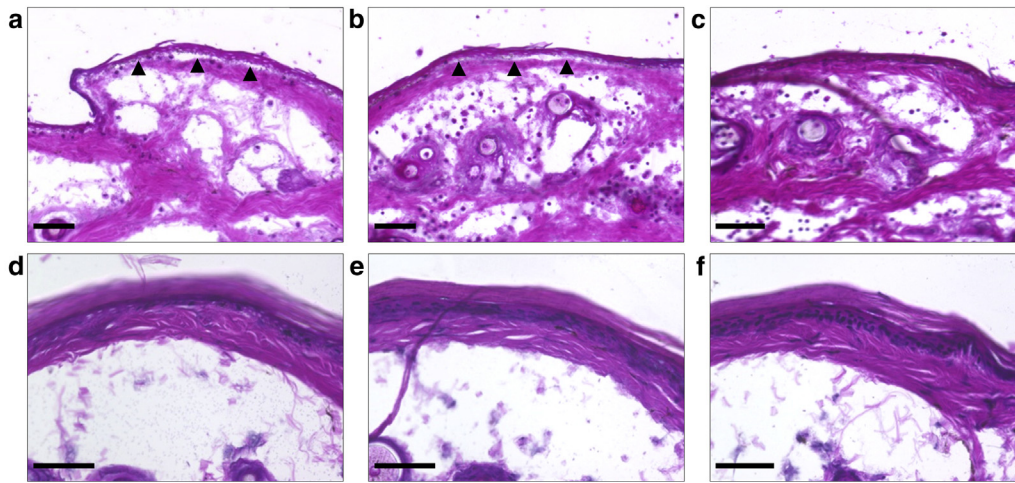


Figure 3. Anti-mLAM α 3 IgG-induced dermal-epidermal separation ex vivo depends on leukocytes. (a–f) Rabbit serum generated against (b) mLAM α 3 but not (c) serum from a preimmune rabbit induces dermal-epidermal separation (arrowheads) when incubated with cryosections of murine skin in the presence of leukocytes. (a) As positive control, rabbit serum raised against mBP180NC15A, the immunodominant epitope in bullous pemphigoid, was used. Without incubation of leukocytes, dermal-epidermal separation cannot be induced by (d) anti-BP180 NC15A and (e) anti-mLAM α 3 serum. (f) Preimmune rabbit serum without leukocyte incubation was used as negative control. Hematoxylin and eosin staining. Scale bars = 50 μ m. mLAM α 3, murine α 3 chain of laminin 332.

two models (Ishii et al., 2011; Liu et al., 1993; Nishie et al., 2007; Schulze et al., 2014; Sitaru et al., 2005; 2006; Woodley et al., 2005) might be explained by the different expression of their target antigens.

We observed a dose-dependent induction of disease activity, reflected by increasing skin and conjunctival lesions and decreasing body weight in response to repeated injections of 1 mg, 3 mg, and 6 mg anti-LAM α 3 IgG (Figure 2a–d). Weight loss correlated with the extent of oral involvement ($R^2 = 0.679$, $P < 0.001$) indicating that the painful oral lesions lead to reduced food uptake (see Supplementary Figure S3 online).

The mouse model reflects major histopathological and immunopathological characteristics of human MMP

Immunopathologically, anti-mLAM α 3, C3, and C5 were localized along the basement membrane of murine skin and various mucosal tissues including buccae, tongue, esophagus, stomach, small intestine, colon, and bladder (Figure 1h, 1i, 1k, 1l, 1n, 1o, and Supplementary Figure S4 online; data for C5 not shown). Linear deposits of C3 at the DEJ of perilesional skin were found in 86% of patients with anti-laminin 332 MMP (Amber et al., 2016). Electron microscopy showed splitting within the lower lamina lucida, as in patients with anti-laminin 332 MMP (see Supplementary Figure S5a–d online).

Lesional histopathology showed subepidermal splitting and a dense neutrophil-rich infiltrate below the basement membrane zone in lesional skin, conjunctiva, and buccal mucosa in nearly all anti-mLAM α 3-injected mice (Figure 1g, 1j, and 1m). To a lesser extent, subepidermal split formation was also seen in the tongue, esophagus, and bladder (see Supplementary Figure S4a, S4d, and S4p). C3 depositions were detected at the basal membrane zone of urothelia in 7 of 11 anti-mLAM α 3-treated mice, with suburothelial splitting in 6 of these 7 animals (see Supplementary Figure S4p, S4r). The lack of split formation in the stomach, small intestine, and colon may be explained by the weaker depositions

of IgG and/or C3 in these tissues or the different processes in mucosal inflammation (see Supplementary Figure S4g–o).

Immunohistochemistry of lesional skin biopsy samples showed neutrophils as predominant inflammatory cells (24% of inflammatory cells), followed by macrophages (21%) and CD3-positive lymphocytes (13%) (see Supplementary Figure S6 online).

In human anti-laminin 332 MMP, histopathology findings are variable. However, most patients suffer from a moderate to dense inflammatory infiltrate predominantly composed of lymphocytes and neutrophils. In some patients, eosinophils and plasma cells can also be found (Egan and Yancey, 2000; Rose et al., 2009). Few patients with only a scant infiltrate were also described. The only study that systematically investigated the histopathology of anti-laminin 332 MMP patients concluded that this entity cannot be differentiated from other pemphigoid diseases such as BP, EBA, and anti-p200 pemphigoid based on histopathology (Rose et al., 2009).

The histopathological findings in the present model are in contrast to findings in the previously reported mouse model of anti-laminin 332 pemphigoid (Lazarova et al., 1996, 2000a, 2000b; Lazarova et al., 1996). The subepidermal splitting devoid of any inflammation was observed with IgG from anti-laminin 332 MMP patients injected in human skin grafted onto the back of SCID mice IgG antibodies and with Fab fragments of rabbit anti-human laminin 332 IgG injected in neonatal BALB/c mice (Lazarova et al., 2000a, 2000b).

IgG against both the middle and C-terminal regions of anti-mLAM α 3 is pathogenic

Repeated injections of IgG affinity purified against the C-terminal and middle portions of mLAM α 3, resulted in similar disease activities (see Supplementary Figure S7 online). No differences in the extent of skin, oral, and conjunctival lesions were noted (see Supplementary Figure S7a–e). In line, deposits of IgG and C3 at the DEJ were not significantly different (Figure S7g–i). These data indicate that pathogenic

epitopes are not restricted to a specific region of mLAM α 3. In contrast, other target antigens in pemphigoid diseases such as BP180 (type XVII collagen) in BP and type VII collagen in EBA harbor well-defined immunodominant regions that mediate the pathogenic effect of autoantibodies (Izumi et al., 2016; Liu et al., 1995a; Nishie et al., 2007; Schmidt et al., 2000; Sitaru et al., 2002b). This notion is supported by the described finding that most anti-laminin 332 MMP patient sera recognize multiple epitopes on LAM α 3. Further studies are needed to explore the pathogenic potential of antibodies against mLAM α 3 and mLAM α 2.

The laminin 332 MMP model is Fc γ R dependent

The striking difference between previous models and the model described here is also reflected by its Fc γ R dependence. The effect of anti-mLAM α 3 IgG to induce subepidermal splitting in cryosections of murine skin depended on the addition of leukocytes from healthy volunteers and was abandoned when the subsequent incubation of skin sections with leukocytes was omitted (Figure 3a–f). In this model, subepidermal splitting induced by anti-type VII collagen IgG in EBA has previously been shown to be mediated by the release of reactive oxygen species and matrix metalloproteinase 9 released from leukocytes that had bound along the DEJ (Shimanovich et al., 2004; Sitaru et al., 2002a).

Further, the strong correlation of the myeloperoxidase activity in the ear skin of diseased mice with the extent of skin lesions measured at day 12 ($R^2 = 0.800$, $P < 0.001$) also suggests a pathogenic relevance of neutrophils in the anti-mLAM α 3 IgG-mediated tissue destruction (see [Supplementary Figure S8](#) online). Third, and most important, Fc γ R chain-deficient mice injected with anti-mLAM α 3 IgG did not develop clinical disease, whereas strong labeling of IgG was observed along the DEJ of skin and mucosal biopsy samples (Figure 4). Fourth, subcutaneous injection of F(ab')₂ fragments of anti-mLAM α 3 IgG in the ears of C57BL/6 mice did not result in subepidermal splitting. An inflammatory dermal infiltrate and skin lesions were absent, and staining at the DEJ was as strong as after injection of anti-mLAM α 3 IgG (Figure 4).

C5aR1 is critically involved in the pathophysiology of experimental murine laminin 332 MMP

Because strong deposits of C3 and C5 were present along the basal membrane zone of perilesional biopsy samples of skin and various mucosal tissues (Figure 1i, 1l, 1o, and [Supplementary Figure S4](#); data for C5 not shown), we finally aimed at exploring the pathophysiological relevance of complement activation in this mouse model.

C5a is the most downstream product of the complement cascade activated by all three complement pathways and is a very powerful chemoattractant that guides neutrophils, monocytes, and macrophages toward sites of complement activation (Ricklin et al., 2010; Zhang et al., 2010). C5a can bind to its two receptors C5aR1 and C5aR2 (previously termed C5L2). Although C5aR1 triggers proinflammatory signals, C5aR2 has more regulatory functions and may act as a decoy receptor (Ricklin et al., 2010; Zhang et al., 2010). We therefore decided to investigate the role of the key proinflammatory C5aR1 in the pathophysiology of our anti-laminin 332 MMP model.

C5aR1-deficient mice showed a significantly reduced disease activity (Figure 5). In C5aR1-deficient compared with wild-type mice, the affected body surface area was 74% lower ($P < 0.001$) (Figure 5b), the body weight score 96% lower (Figure 5c), the conjunctival involvement 88% lower ($P < 0.0001$) (Figure 5d), and the cumulative disease score 90% lower ($P < 0.001$; Figure 5e). Of note, microscopic subepidermal blisters and a neutrophil-rich inflammatory infiltrate, although less dense compared with those of wild-type animals, was observed in six of eight C5aR1-deficient mice (Figure 5g). These data are in line with the strong role of C5aR1 in experimental models of two other pemphigoid diseases, BP and EBA (Heimbach et al., 2011; Karsten et al., 2012; Liu et al., 1995b).

The importance of the Fc γ R and, to a lesser extent, C5aR1 in the mouse model established here is in accordance with the observed dense inflammatory infiltrate that may be attracted via these receptors. In contrast, previous experiments with neonatal C5-deficient DBA/2Ncr mice subjected to anti-human laminin 332 IgG resulted in the same disease activity and the same extent of noninflammatory subepidermal blisters compared with wild-type mice (Lazarova et al., 1996). Although the presence of conjunctival lesions and a dense inflammatory infiltrate in the present model closely reflect the human situation, the use of IgG against mLAM α 3 and adult mice (instead of IgG against all subunits of human laminin 332 and neonatal mice) may explain the clinical and immunopathological differences between the two animal models of anti-laminin 332 MMP.

In summary, anti-laminin 332 MMP is a prototypic organ-specific autoantibody-mediated disease. The mouse model described here mirrors major clinical and immunopathological features of the human disease, that is, oral, pharyngeal, esophageal, and conjunctival lesions; subepidermal blistering with an inflammatory infiltrate below the basement membrane zone; and deposits of IgG, C3, and C5 along the basement membrane zone. The anti-laminin 332 MMP mouse model will be helpful to further dissect the pathophysiology of this disorder and explore the effect of more specific anti-inflammatory mediators on mucosal and skin lesions.

MATERIALS AND METHODS

Mice

C57BL/6, Fc γ R^{-/-} (B6;129P2-Fc γ R1^{tm1Rav}/J), and C5aR1^{-/-} on C57BL/6 background were bred and housed in a 12-hour light-dark cycle at the animal facility of the University of Lübeck. All experiments were performed on mice anesthetized by intraperitoneal administration of a mixture of ketamine (100 μ g/g) and xylazine (15 μ g/g). Animal experiments were approved by the Animal Care and Use Committee of Schleswig-Holstein (95-7/13, 40-3/15).

Epitope mapping of human LAM α 3

Epitope mapping of human LAM α 3 is discussed in the [Supplementary Materials](#) (see [Supplementary Figure S1](#), [Supplementary Table S1](#) online).

Expression and purification of murine LAM α 3 fragments

Two fragments of the mLAM α 3 (accession number NM_010680.1), middle (1,002 base pairs, aa1656–1985) and C-terminal (1,740 base pairs, aa2756–3330) portions, were generated and optimized for

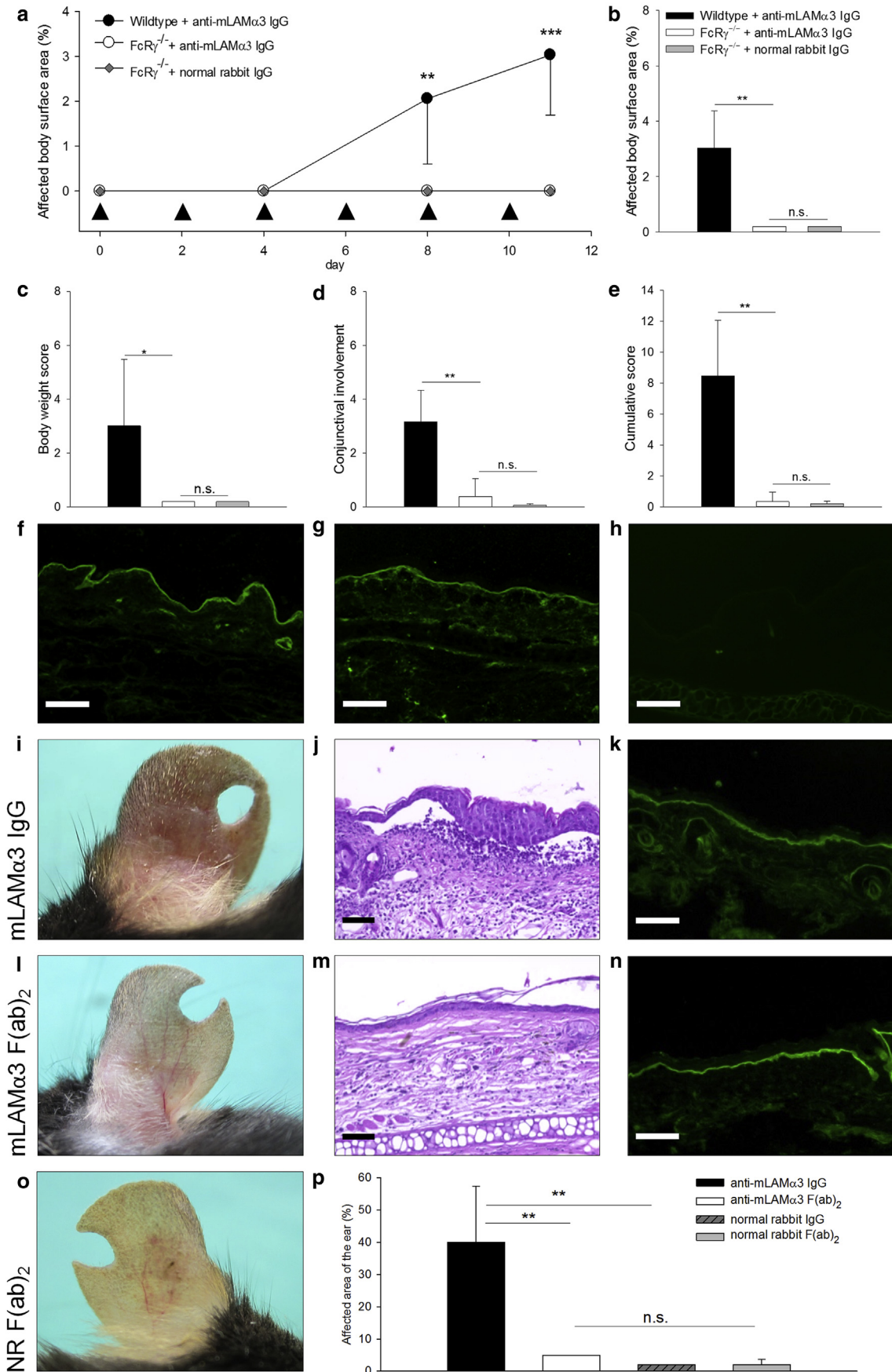


Figure 4. FcR γ are essential in anti-mLAM α 3 IgG-mediated tissue destruction. (a) Mice lacking the activating γ chain of the FcR (FcR $\gamma^{-/-}$) are completely protected from the pathogenic effect of anti-mLAM α 3 IgG. FcR $\gamma^{-/-}$ (n = 8) and matched wild-type mice were injected with 5 mg mLAM α 3 IgG (n = 5) and

expression in *Escherichia coli* (Thermo Fisher, Darmstadt Germany). Middle and C-terminal mLAM α 3 were each cloned into expression vector pRSET_A_A185. Both fragments were expressed as His-fusion proteins in *E. coli* and purified by metal affinity chromatography on TALON superflow (Clontech, Palo Alto, CA). Protein concentrations were measured with Coomassie Brilliant Blue stained SDS-PAGE, using bovine serum albumin as the protein standard.

Rabbit IgG

New Zealand white rabbits were immunized with a mixture of recombinant His-tagged fragments middle and C-terminal mLAM α 3 portions. Total rabbit IgG was purified by affinity chromatography using protein G Sepharose (Genscript, Piscataway, NJ). Antigen-specific IgG was purified using the recombinant fragments coupled to NHS-activated Sepharose (GE Healthcare, Munich, Germany).

Anti-mLAM α 3 F(ab')₂ fragments were generated by pepsin digestion (Thermo Scientific, Rockford, IL) according to the manufacturer's instructions and isolated by affinity chromatography using protein G Sepharose. IgG fragments were screened by SDS-PAGE under reduced and nonreduced conditions. F(ab')₂-fragments from normal rabbit IgG were prepared similarly. Normal rabbit serum was obtained from PAN-Biotech (Aidenbach, Germany). The recombinant forms of mLAM α 3, mid and c-term, were applied to affinity-purify mid-specific and c-term-specific IgG from anti-mLAM α 3 rabbit serum detailed in the [Supplementary Materials](#).

Cryosection assay

The leukocyte-activating capacity of anti-mLAM α 3 serum was evaluated ex vivo on cryosections of murine skin, as reported previously (see [Supplementary Materials](#)) (Sitaru et al., 2002b).

Immunoblotting

Immunoblotting was performed as previously described (see [Supplementary Materials](#)) (Schulze et al., 2014; Vafia et al., 2012).

Antibody transfer mouse model

Purified rabbit anti-mLAM α 3 IgG or normal rabbit IgG was repetitively injected subcutaneously into the neck of mice every second day for 12 days (Figures 4a, 5a). IgG doses ranged between 1.0 and 7.5 mg/injection and are specified for each experiment in the respective figure legends. Anti-mid and anti-c-term mLAM α 3 IgG was injected accordingly in doses with equal anti-DEJ titers of 0.5 (mid) and 1 mg/injection (c-term). On day 12, mice were killed, and samples were taken for further analysis unless stated otherwise. The scoring is detailed in the [Supplementary Materials](#).

In the local antibody transfer model, 500 μ g of IgG or 400 μ g of F(ab')₂-fragments (a roughly equimolar dose compared with the intact IgG injections), were injected subcutaneously into the ear of mice. 48 hours after injection the percentage of affected ear skin was scored, and ear samples were taken for further analysis.

Endoscopy

High-resolution mouse endoscopy of the oral cavity was used (HOPKINS Optik 64019BA; Karl StorzAidaVet, Tuttlingen, Germany) to determine the extent of oral lesions.

Immunofluorescence microscopy and histopathology

Direct and indirect immunofluorescence microscopy and hematoxylin and eosin staining were performed according to standard protocols described previously (see [Supplementary Materials](#)) (Schulze et al., 2014; Vafia et al., 2012).

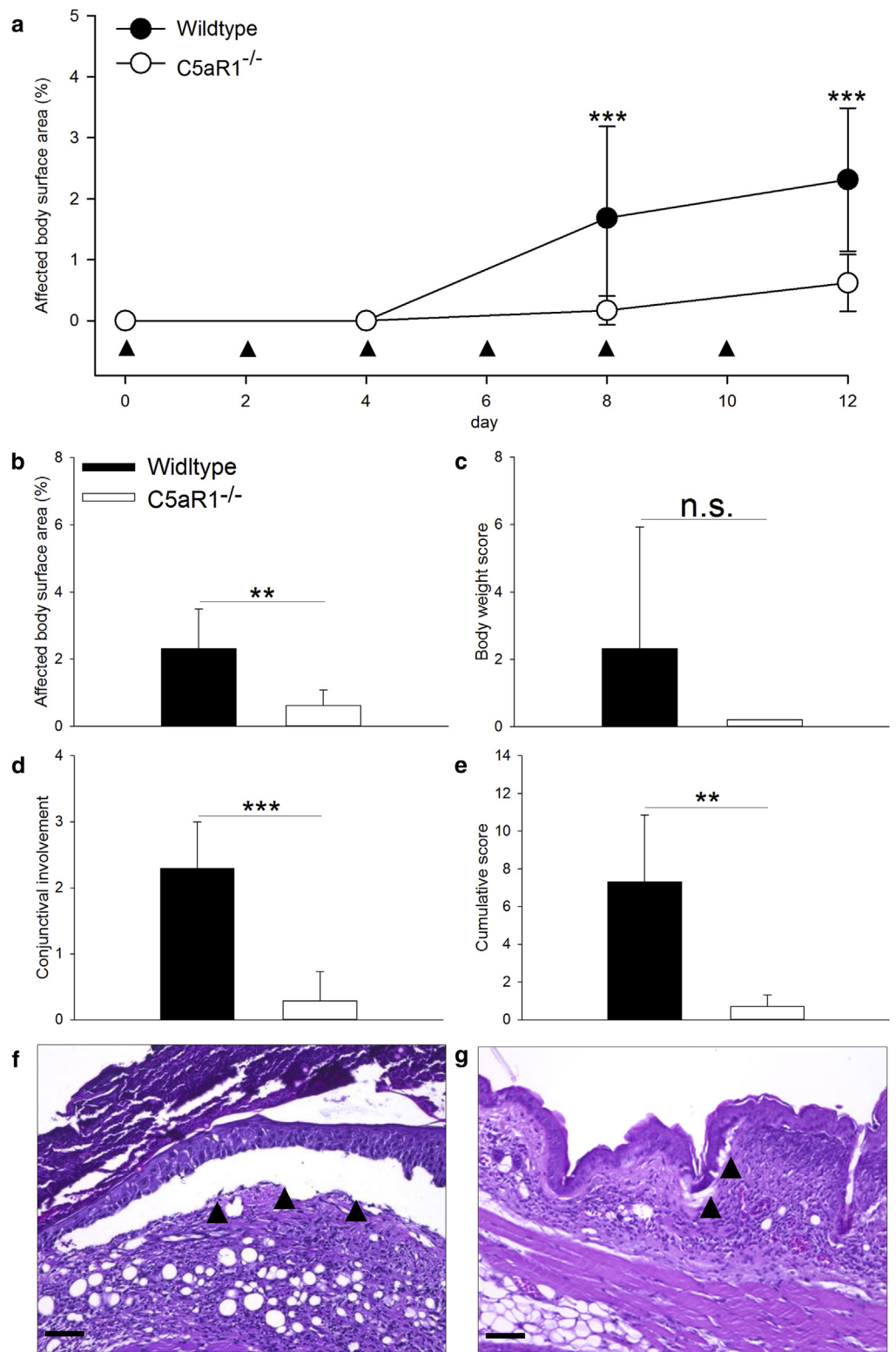
For immunostaining of infiltrating cells, cryosections of murine skin biopsy samples were blocked with 3% bovine serum albumin in Tris-buffered saline. All following washing steps were performed three times for 5 minutes in phosphate buffered saline-Tween (0.05% Tween). For staining of neutrophils, biotin anti-mouse Ly-6G antibody (clone 1A8) with rat IgG 2 κ (clone RTK2758) as isotype control (1:400; Biolegend, Fell, Germany) were used. T cells were stained with biotin anti-mouse CD3 ϵ antibody (clone 145-2C11) and biotin Armenian hamster IgG isotype control antibody (clone HTK888; 1:100; Biolegend). For the visualization of macrophages/monocytes, anti-mouse F4/80 antibody (Clone A3-1; 1:700; Bio-Rad) and isotype IgG2b (Clone R12-3; 1:700; BD Pharmingen, Heidelberg, Germany) were used with biotin goat anti-rat IgG (1:800; Biolegend) as the secondary antibody. As a detection agent, Daylight 594-conjugated streptavidin (1:200; Thermo Fisher) was applied. Additional DAPI staining was performed for all sections. Specimens were mounted in Fluoromount-G (Southern Biotech, Birmingham, AL) and kept at -20 °C. Cell numbers were determined by counting the specific cells in relation to DAPI-positive cells in three visual fields with a field size of 115 μ m².

Electron microscopy

Indirect immunogold electron microscopy was performed to characterize the exact binding site of rabbit anti-mLAM α 3 serum in normal murine skin as previously described (Ishiko et al., 1993). Samples for transmission electron microscopy were taken from lesional skin of mice injected with anti-mLAM α 3 IgG. Fixed samples were processed as described (Ishiko and Shimizu, 2001). Stained

FcR γ ^{-/-} mice with 5 mg of NR IgG (n = 3) on days 0, 2, 4, 6, 8, and 10 (arrowheads). On all evaluated days (days 4, 8, and 11) no skin lesions were seen in either FcR γ ^{-/-} mice injected with anti-mLAM α 3 IgG and, as expected, FcR γ ^{-/-} mice injected with NR IgG. (b–e) When (b) skin lesions, (c) body weight score, (d) conjunctival involvement, and (e) the cumulative disease score during the course of the entire experiment were analyzed, significant differences were seen between the FcR γ ^{-/-} mice and wild-type mice injected with anti-mLAM α 3 IgG but not between the FcR γ ^{-/-} mice injected with anti-mLAM α 3 IgG and FcR γ ^{-/-} control mice injected with NR IgG. (a) Two-way analysis of variance, bars show mean – standard deviation, (b–e) one-way analysis of variance of area under the curve, bars show mean + standard deviation, with Holm-Sidak posttest when analysis of variance was significant. *P < 0.01, **P < 0.001, ***P < 0.0001. (f–h) Direct IF microscopy of perilesional skin biopsy samples taken on day 11 show the same extent of IgG staining along the dermal-epidermal junction in (g) FcR γ ^{-/-} mice and (f) wild-type mice injected with anti-mLAM α 3 IgG. (h) As expected, no labeling is present in FcR γ ^{-/-} mice injected with NR IgG. (i, j, l, m–p) In contrast to ears of C57BL/6 mice injected with mLAM α 3 IgG (500 μ g, n = 3), ears injected with mLAM α 3 IgG F(ab')₂ fragments (400 μ g, n = 3) do not show clinical and histopathological disease after 48 hours. Ears of C57BL/6 mice (n = 3) injected with 500 μ g of NR IgG and 400 μ g NR F(ab')₂ fragments (n = 3) served as negative controls. (k, n) Direct IF microscopy of perilesional biopsy samples of ear skin. IgG along the basal membrane zone shows the same staining intensity in ears injected with mLAM α 3 IgG F(ab')₂ fragments compared with ears injected with mLAM α 3 IgG. (p) Clinical involvement of ear skin. When the disease course during the entire experiment was analyzed, ears injected with mLAM α 3 IgG were significantly more affected compared with ears injected with mLAM α 3 IgG F(ab')₂, NR IgG, and NR F(ab')₂ IgG, respectively (one-way analysis of variance, bars show mean + standard deviation, with Holm-Sidak posttest when analysis of variance was significant). **P < 0.001. Scale bars = 50 μ m. IF, immunofluorescence; mLAM α 3, murine α 3 chain of laminin 332; NR, normal rabbit; n.s., not significant.

Figure 5. C5aR1^{-/-} mice injected with anti-mLAMα3 IgG showed reduced disease activity. (a) C5aR1^{-/-} (n = 8) and wild-type mice (C57BL/6, n = 8) were injected subcutaneously with 4 mg/mouse mLAMα3 IgG on days 0, 2, 4, 6, 8, and 10. (a, b) In C5aR1^{-/-} mice, the affected body surface area was significantly smaller compared with wild-type mice both (a) during the course of the disease (two-way analysis of variance) and (b) at the end of the experiment on day 12 (*t* test). (c–e) When the disease course during the entire experiment was analyzed, C5aR1^{-/-} mice also showed (c) a significantly reduced body weight score, (d) conjunctival involvement, and (e) cumulative disease score (all area under the curve; all *t* test). Bars show (a) mean – standard deviation and (b–e) mean + standard deviation. ***P* < 0.001; ****P* < 0.0001. (f, g) Hematoxylin and eosin staining of (f) lesional ear skin of wild-type and (g) C5aR1^{-/-} mice. Although subepidermal splitting (arrowheads) was more pronounced and the inflammatory dermal infiltrate denser in the wild-type mice, C5aR1^{-/-} mice also showed clear subepidermal splitting and infiltration of neutrophils and macrophages in the upper dermis. Scale bars = 50 μm. mLAMα3, murine α3 chain of laminin 332; n.s., not significant.



sections were examined using an electron microscope (Model JEOLJEM-1230; JEOL, Tokyo, Japan).

Neutrophil-specific myeloperoxidase activity

Neutrophil infiltration in murine skin was quantified by determination of myeloperoxidase activity in homogenized ear specimens as described (Hammers et al., 2011). Myeloperoxidase content was

expressed as units of MPO activity per milligram of protein. Protein concentration was assessed using BCA assay (Thermo Scientific, Rockford, IL).

Statistics

Differences in disease severity were determined by *t* test, one-way analysis of variance, or two-way analysis of variance. For

correlation analysis Pearson product moment correlation was applied. Data are presented as mean \pm standard deviation. A *P*-value less than 0.05 was considered statistically significant.

CONFLICT OF INTEREST

The authors state no conflict of interest.

ACKNOWLEDGMENTS

We are grateful to Vanessa Krull, Lübeck, for excellent technical support. The study was supported by Deutsche Forschungsgemeinschaft through the Research Training Group 1727 *Modulation of Autoimmunity* (to ES), the Clinical Research Unit 303 *Pemphigoid Diseases* (to ES, SCHM 1686/7-1), and the Schleswig-Holstein Cluster of Excellence *Inflammation at Interfaces* (EXC 306/2) and the University of Lübeck (to FSS).

SUPPLEMENTARY MATERIAL

Supplementary material is linked to the online version of the paper at www.jidonline.org, and at <http://dx.doi.org/10.1016/j.jid.2017.03.037>.

REFERENCES

- Amber KT, Bloom R, Hertl M. A systematic review with pooled analysis of clinical presentation and immunodiagnostic testing in mucous membrane pemphigoid: association of anti-laminin-332 IgG with oropharyngeal involvement and the usefulness of ELISA. *J Eur Acad Dermatol Venereol* 2016;30:72–7.
- Bernard P, Antonicelli F, Bedane C, Joly P, Le Roux-Villet C, Duvert-Lehembre S, et al. Prevalence and clinical significance of anti-laminin 332 autoantibodies detected by a novel enzyme-linked immunosorbent assay in mucous membrane pemphigoid. *JAMA Dermatol* 2013;149:533–40.
- Bernard P, Prost C, Durepaire N, Basset-Seguain N, Didierjean L, Saurat JH. The major cicatricial pemphigoid antigen is a 180-kD protein that shows immunologic cross-reactivities with the bullous pemphigoid antigen. *J Invest Dermatol* 1992;99:174–9.
- Bernard P, Vaillant L, Labelle B, Bedane C, Arbeille B, Denoex JP, et al. Incidence and distribution of subepidermal autoimmune bullous skin diseases in three French regions. Bullous Diseases French Study Group. *Arch Dermatol* 1995;131:48–52.
- Bertram F, Brocker EB, Zillikens D, Schmidt E. Prospective analysis of the incidence of autoimmune bullous disorders in Lower Franconia, Germany. *J Dtsch Dermatol Ges* 2009;7:434–40.
- Borradori L, Sonnenberg A. Structure and function of hemidesmosomes: more than simple adhesion complexes. *J Invest Dermatol* 1999;112:411–8.
- Chan LS, Ahmed AR, Anhalt GJ, Bernauer W, Cooper KD, Elder MJ, et al. The first international consensus on mucous membrane pemphigoid: definition, diagnostic criteria, pathogenic factors, medical treatment, and prognostic indicators. *Arch Dermatol* 2002;138:370–9.
- Domloge-Hultsch N, Anhalt GJ, Gammon WR, Lazarova Z, Briggaman RA, Welch M, et al. Antiepiligrin cicatricial pemphigoid. A subepithelial bullous disorder. *Arch Dermatol* 1994;130:1521–9.
- Domloge-Hultsch N, Gammon WR, Briggaman RA, Gil SG, Carter WG, Yancey KB. Epiligrin, the major human keratinocyte integrin ligand, is a target in both an acquired autoimmune and an inherited subepidermal blistering skin disease. *J Clin Invest* 1992;90:1628–33.
- Egan CA, Lazarova Z, Darling TN, Yee C, Cote T, Yancey KB. Anti-epiligrin cicatricial pemphigoid and relative risk for cancer. *Lancet* 2001;357:1850–1.
- Egan CA, Yancey KB. The clinical and immunopathological manifestations of anti-epiligrin cicatricial pemphigoid, a recently defined subepithelial autoimmune blistering disease. *Eur J Dermatol* 2000;10:585–9.
- Fine JD, Bruckner-Tuderman L, Eady RA, Bauer EA, Bauer JW, Has C, et al. Inherited epidermolysis bullosa: updated recommendations on diagnosis and classification. *J Am Acad Dermatol* 2014;70:1103–26.
- Hamill KJ, Paller AS, Jones JC. Adhesion and migration, the diverse functions of the laminin alpha3 subunit. *Dermatologic clinics* 2010;28:79–87.
- Hammers CM, Bieber K, Kalies K, Banczyk D, Ellebrecht CT, Ibrahim SM, et al. Complement-fixing anti-type VII collagen antibodies are induced in Th1-polarized lymph nodes of epidermolysis bullosa acquisita-susceptible mice. *J Immunol* 2011;187:5043–50.
- Heimbach L, Li Z, Berkowitz P, Zhao M, Li N, Rubenstein DS, et al. The C5a receptor on mast cells is critical for the autoimmune skin-blistering disease bullous pemphigoid. *J Biol Chem* 2011;286:15003–9.
- Higgins GT, Allan RB, Hall R, Field EA, Kaye SB. Development of ocular disease in patients with mucous membrane pemphigoid involving the oral mucosa. *Br J Ophthalmol* 2006;90:964–7.
- Hsu R, Lazarova Z, Yee C, Yancey KB. Noncomplement fixing, IgG4 autoantibodies predominate in patients with anti-epiligrin cicatricial pemphigoid. *J Invest Dermatol* 1997;109:557–61.
- Hübner F, Recke A, Zillikens D, Linder R, Schmidt E. Prevalence and age distribution of pemphigus and pemphigoid diseases in Germany. *J Invest Dermatol* 2016;136:2495–8.
- Ishii N, Recke A, Mihai S, Hirose M, Hashimoto T, Zillikens D, et al. Autoantibody-induced intestinal inflammation and weight loss in experimental epidermolysis bullosa acquisita. *J Pathol* 2011;224:234–44.
- Ishiko A, Shimizu H. Electron microscopy in diagnosis of autoimmune bullous disorders. *Clin Dermatol* 2001;19:631–7.
- Ishiko A, Shimizu H, Kikuchi A, Ebihara T, Hashimoto T, Nishikawa T. Human autoantibodies against the 230-kD bullous pemphigoid antigen (BPAG1) bind only to the intracellular domain of the hemidesmosome, whereas those against the 180-kD bullous pemphigoid antigen (BPAG2) bind along the plasma membrane of the hemidesmosome in normal human and swine skin. *J Clin Invest* 1993;91:1608–15.
- Izumi K, Nishie W, Mai Y, Wada M, Natsuga K, Ujii H, et al. Autoantibody Profile Differentiates between Inflammatory and Noninflammatory Bullous Pemphigoid. *J Invest Dermatol* 2016;136:2201–10.
- Karsten CM, Pandey MK, Figge J, Kilchenstein R, Taylor PR, Rosas M, et al. Anti-inflammatory activity of IgG1 mediated by Fc galactosylation and association of FcγRIIb and Dectin-1. *Nat Med* 2012;18:1401–6.
- Kirtschig G, Marinkovich MP, Burgesson RE, Yancey KB. Anti-basement membrane autoantibodies in patients with anti-epiligrin cicatricial pemphigoid bind the alpha subunit of laminin 5. *J Invest Dermatol* 1995;105:543–8.
- Lazarova Z, Hsu R, Briggaman RA, Yancey KB. Fab fragments directed against laminin 5 induce subepidermal blisters in neonatal mice. *Clin Immunol* 2000a;95:26–32.
- Lazarova Z, Hsu R, Yee C, Yancey KB. Human anti-laminin 5 autoantibodies induce subepidermal blisters in an experimental human skin graft model. *J Invest Dermatol* 2000b;114:178–84.
- Lazarova Z, Sadler E, Salato VK, Lopez A, Yancey K. Development and characterization of a passive transfer animal model of acute and chronic ocular cicatricial pemphigoid (abstract). *J Invest Dermatol* 2007;127:S5.
- Lazarova Z, Yee C, Darling T, Briggaman RA, Yancey KB. Passive transfer of anti-laminin 5 antibodies induces subepidermal blisters in neonatal mice. *J Clin Invest* 1996;98:1509–18.
- Lazarova Z, Yee C, Lazar J, Yancey KB. IgG autoantibodies in patients with anti-epiligrin cicatricial pemphigoid recognize the G domain of the laminin 5 alpha-subunit. *Clin Immunol* 2001;101:100–5.
- Leverkus M, Schmidt E, Lazarova Z, Brocker EB, Yancey KB, Zillikens D. Antiepiligrin cicatricial pemphigoid: an underdiagnosed entity within the spectrum of scarring autoimmune subepidermal bullous diseases? *Arch Dermatol* 1999;135:1091–8.
- Liu Z, Diaz LA, Swartz SJ, Troy JL, Fairley JA, Giudice GJ. Molecular mapping of a pathogenically relevant BP180 epitope associated with experimentally induced murine bullous pemphigoid. *J Immunol* 1995a;155:5449–54.
- Liu Z, Diaz LA, Troy JL, Taylor AF, Emery DJ, Fairley JA, et al. A passive transfer model of the organ-specific autoimmune disease, bullous pemphigoid, using antibodies generated against the hemidesmosomal antigen, BP180. *J Clin Invest* 1993;92:2480–8.
- Liu Z, Giudice GJ, Swartz SJ, Fairley JA, Till GO, Troy JL, et al. The role of complement in experimental bullous pemphigoid. *J Clin Invest* 1995b;95:1539–44.
- Nishie W, Sawamura D, Goto M, Ito K, Shibaki A, McMillan JR, et al. Humanization of autoantigen. *Nat Med* 2007;13:378–83.
- Oyama N, Setterfield JF, Powell AM, Sakuma-Oyama Y, Albert S, Bhogal BS, et al. Bullous pemphigoid antigen II (BP180) and its soluble extracellular domains are major autoantigens in mucous membrane pemphigoid: the pathogenic relevance to HLA class II alleles and disease severity. *Br J Dermatol* 2006;154:90–8.

- Ricklin D, Hajishengallis G, Yang K, Lambris JD. Complement: a key system for immune surveillance and homeostasis. *Nat Immunol* 2010;11:785–97.
- Rose C, Schmidt E, Kerstan A, Thoma-Uszynski S, Wesselmann U, Kasbohrer U, et al. Histopathology of anti-laminin 5 mucous membrane pemphigoid. *J Am Acad Dermatol* 2009;61:433–40.
- Schmidt E, Obe K, Brocker EB, Zillikens D. Serum levels of autoantibodies to BP180 correlate with disease activity in patients with bullous pemphigoid. *Arch Dermatol* 2000;136:174–8.
- Schmidt E, Skrobek C, Kromminga A, Hashimoto T, Messer G, Brocker EB, et al. Cicatricial pemphigoid: IgA and IgG autoantibodies target epitopes on both intra- and extracellular domains of bullous pemphigoid antigen 180. *Br J Dermatol* 2001;145:778–83.
- Schmidt E, Zillikens D. Pemphigoid diseases. *Lancet* 2013;381:320–32.
- Schulze FS, Beckmann T, Nimmerjahn F, Ishiko A, Collin M, Kohl J, et al. Fcγ receptors III and IV mediate tissue destruction in a novel adult mouse model of bullous pemphigoid. *Am J Pathol* 2014;184:2185–96.
- Shimanovich I, Mihai S, Oostingh GJ, Ilenchuk TT, Brocker EB, Opendakker G, et al. Granulocyte-derived elastase and gelatinase B are required for dermal-epidermal separation induced by autoantibodies from patients with epidermolysis bullosa acquisita and bullous pemphigoid. *J Pathol* 2004;204:519–27.
- Sitaru C, Chiriac MT, Mihai S, Buning J, Gebert A, Ishiko A, et al. Induction of complement-fixing autoantibodies against type VII collagen results in subepidermal blistering in mice. *J Immunol* 2006;177:3461–8.
- Sitaru C, Kromminga A, Hashimoto T, Brocker EB, Zillikens D. Autoantibodies to type VII collagen mediate Fcγ-dependent neutrophil activation and induce dermal-epidermal separation in cryosections of human skin. *Am J Pathol* 2002a;161:301–11.
- Sitaru C, Mihai S, Otto C, Chiriac MT, Hausser I, Dotterweich B, et al. Induction of dermal-epidermal separation in mice by passive transfer of antibodies specific to type VII collagen. *J Clin Invest* 2005;115:870–8.
- Sitaru C, Schmidt E, Petermann S, Munteanu LS, Brocker EB, Zillikens D. Autoantibodies to bullous pemphigoid antigen 180 induce dermal-epidermal separation in cryosections of human skin. *J Invest Dermatol* 2002b;118:664–71.
- Vafia K, Groth S, Beckmann T, Hirose M, Dworschak J, Recke A, et al. Pathogenicity of autoantibodies in anti-p200 pemphigoid. *PLoS One* 2012;7:e41769.
- Woodley DT, Chang C, Saadat P, Ram R, Liu Z, Chen M. Evidence that anti-type VII collagen antibodies are pathogenic and responsible for the clinical, histological, and immunological features of epidermolysis bullosa acquisita. *J Invest Dermatol* 2005;124:958–64.
- Yamamoto K, Inoue N, Masuda R, Fujimori A, Saito T, Imajoh-Ohmi S, et al. Cloning of hamster type XVII collagen cDNA, and pathogenesis of anti-type XVII collagen antibody and complement in hamster bullous pemphigoid. *J Invest Dermatol* 2002;118:485–92.
- Zhang X, Schmutte I, Laumonier Y, Pandey MK, Clark JR, König P, et al. A critical role for C5L2 in the pathogenesis of experimental allergic asthma. *J Immunol* 2010;185:6741–52.